Distributed Secondary Frequency Control through MTDC Transmission Systems

Martin Andreasson*, Roger Wiget, Dimos V. Dimarogonas, Karl H. Johansson and Göran Andersson

***Abstract*—In this paper, we present distributed controllers for sharing primary and secondary frequency control reserves for asynchronous AC transmission systems, which are connected through a multi-terminal HVDC grid. By using passivity arguments, the equilibria of the closed-loop system are shown to be globally asymptotically stable. We quantify the static errors of the voltages and frequencies, and give upper bounds for these errors. It is also shown that the controllers have the property of power sharing, i.e., primary and secondary frequency control reserves are shared fairly amongst the AC systems. The proposed controllers are applied to a high-order dynamic model of of a power system consisting of asynchronous AC grids connected through a 6-terminal HVDC grid.**

I. Introduction

Transmitting power over long distances with minimal losses is one of the greatest challenges in today's power transmission systems. The strong rising share of renewables increased the distances between power generation and consumption. This is a driving factor behind the development of long-distance power transmission technologies. One such example are large-scale off-shore wind farms, which often require power to be transmitted in cables over long distances to the mainland power grid [4]. Due to the high resistive losses in AC cables, high-voltage direct current (HVDC) power transmission is a commonly used technology for power transmission in these cases. The higher investment cost of an HVDC transmission system compared to an AC transmission system, is compensated by the lower resistive losses for sufficiently long distances [14]. The break-even point, i.e., the point where the total construction and operation costs of overhead HVDC and AC lines are equal, is typically 500–800 km [16]. However, for cables, the break-even point is typically less than 50 km [19]. Increased use of HVDC technologies for electrical power transmission suggests that future HVDC transmission systems are likely to consist of multiple terminals connected by several HVDC transmission lines [9]. Such systems are referred to as Multi-terminal HVDC (MTDC) systems in the literature.

Maintaining an adequate DC voltage is the single most important practical control problem for HVDC transmission systems. If the DC voltage deviates too far from the nominal operational voltage, equipment could be damaged, resulting in loss of power transmission capability and high costs.

Many existing AC grids are connected through HVDC links, which are typically used for bulk power transfer between AC areas. The fast operation of the DC converters, however, also enables frequency regulation of one of the connected AC grids through the HVDC link. One practical example of this is the island of Gotland in Sweden, which is only connected to the Nordic grid through an HVDC cable [3]. However, since the Nordic grid has orders of magnitudes higher inertia than the AC grid of Gotland, the influence of the frequency regulation on the Nordic grid is negligible. By connecting several AC grids by an MTDC system, primary frequency regulation reserves may be shared, which reduces the need for frequency regulation reserves in the individual AC systems [12]. In [6], distributed control algorithms have been applied to share primary frequency control reserves of asynchronous AC transmission systems connected through an MTDC system. However, the proposed controller requires a slack bus to control the DC voltage, defeating the purpose of distributing the primary frequency regulation reserves. In [1], distributed controllers for secondary voltage control of MTDC systems are proposed, which do not rely on a slack bus. The analysis in the aforementioned reference is however restricted to the dynamics of the MTDC system, thus neglecting any dynamics of connected AC systems.

In [7] and [17], decentralized controllers are employed to share primary frequency control reserves. In [17] no stability analysis of the closed-loop system is performed, whereas [7] guarantees stability provided that the connected AC areas have identical parameters and the voltage dynamics of the HVDC system are neglected. In [18], optimal decentralized controllers for AC systems connected by HVDC systems are derived. In contrast to the aforementioned references, [2] also considers the dynamics of connected AC systems as well as the dynamics of the MTDC system. A distributed controller, relying on a communication network, is proposed in [5]. Stability is guaranteed in the absence of communication delays. The voltage dynamics of the MTDC system are however neglected. Moreover the implementation of the controller requires every controller to access measurements of the DC voltages of all terminals.

In this paper we present two distributed controllers for combined primary and secondary frequency control of asynchronous AC systems connected through an MTDC system.

M. Andreasson, D. V. Dimarogonas and K. H. Johansson are with the ACCESS Linnaeus Centre, KTH Royal Institute of Technology, Stockholm, Sweden. R. Wiget and G. Andersson are with the Power Systems Laboratory, ETH Zurich, Zurich, Switzerland. This work was supported in part by the European Commission, the Swedish Research Council (VR) and the Knut and Alice Wallenberg Foundation. * Corresponding author (mandreas@kth.se).

The first controller requires that the communication network constitutes a complete graph, while the second controller only relies on local information from neighboring AC systems. In contrast to existing controllers in the literature, the proposed controllers in this paper consider the voltage dynamics of the MTDC system, in addition to the frequency dynamics of the AC systems. The equilibrium of the closed-loop system is shown to be globally asymptotically stable for any set of controller parameters. We furthermore bound the asymptotic errors of the voltages and frequencies at the equilibrium, and show the achievable performance is better than for the corresponding decentralized controller studied in [2]. We also show that the frequency control reserves are asymptotically shared approximately equally, which is referred to as power sharing in the literature.

The remainder of this paper is organized as follows. In Section II, the mathematical notation is defined. In Section III, the system model and the control objectives are defined. In Section IV, we recall the decentralized proportional controller for distributing primary frequency control proposed in [2]. In Section V, two secondary frequency controllers for sharing primary and secondary frequency control reserves are presented. In Section VI, simulations of the distributed controller on a four-terminal MTDC test system are provided, showing the effectiveness of the proposed controller. The paper ends with concluding remarks in Section VII.

II. Preliminaries

Let $\mathcal{G}$ be a static, undirected graph. Denote by $\mathcal{V} = \{1, \dots, n\}$ the vertex set of $\mathcal{G}$, and by $\mathcal{E} = \{1, \dots, m\}$ the edge set of $\mathcal{G}$. Let $\mathcal{N}_i$ be the set of neighboring vertices to $i \in \mathcal{V}$. Denote by $\mathcal{B}$ the vertex-edge incidence matrix of $\mathcal{G}$, and let $\mathcal{L}_{\mathcal{W}} = \mathcal{B}W\mathcal{B}^T$ be the weighted Laplacian matrix of $\mathcal{G}$, with edge-weights given by the elements of the diagonal matrix W. We denote the space of real-valued $n \times n$-valued matrices by $\mathbb{R}^{n\times m}$. Let $\mathbb{C}^-$ denote the open left half complex plane, and $\bar{\mathbb{C}}^-$ its closure. We denote by $c_{n\times m}$ a vector or matrix of dimension $n \times m$, whose elements are all equal to c. For a symmetric matrix A, $A > 0$ ($A \geq 0$) is used to denote that A is positive (semi) definite. I_n denotes the identity matrix of dimension n. For simplicity, we will often drop the notion of time dependence of variables, i.e., $x(t)$ will be denoted x. Let $\|\cdot\|_\infty$ denote the maximal absolute value of the elements of a vector.

III. Model and problem setup

We will here give a unified model for an MTDC system interconnected with several asynchronous AC systems. We consider an MTDC transmission system consisting of n converters, each connecting to an AC system, denoted $1, \dots, n$. The converters are assumed to be connected by an MTDC transmission grid. The dynamics of converter i is assumed to be given by

$$C_i\dot{V}_i = -\sum_{j\in\mathcal{N}_i} \frac{1}{R_{ij}}(V_i - V_j) + I_i^{\text{inj}}, \tag{1}$$

where V_i is the voltage of converter i, $C_i > 0$ is its capacitance, and I_i^{inj} is the injected current from an AC grid connected to the DC converter. The constant R_{ij} denotes the resistance of the HVDC transmission line connecting the converters i and j. The graph corresponding to the HVDC line connections is assumed to be connected. The AC system is assumed to consist of a single generator which is connected to the corresponding DC converter, representing an aggregate model of the AC grid. The dynamics of the AC system are given by the swing equation [13]:

$$m_i\dot{\omega}_i = P_i^{\text{gen}} + P_i^{\text{nom}} + P_i^m - P_i^{\text{inj}}, \tag{2}$$

where $m_i > 0$ is its moment of inertia. The constant P_i^{nom} is the nominal generated power, P_i^m is the uncontrolled deviation from the nominal generated power, P_i^{inj} is the power injected to the DC system through the convertera, P_i^{gen} is the generated power by the generation control (primary or secondary) of generator i, respectively. The control objective can now be stated as follows.

Objective 1. *The generation control action should be asymptotically distributed fairly amongst the generators, i.e.,*

$$\lim_{t\to\infty}\left| P_i^{gen}(t) + \frac{1}{n}\sum_{i=1}^{n} P_i^m \right| \leq e^{gen} \quad \forall i = 1, \dots, n,$$

where e^{gen} is a given scalar. Furthermore, the frequencies of the AC systems, as well as the converter voltages, should not deviate too far from their nominal values, i.e.,

$$\lim_{t\to\infty} |V_i(t) - V_i^{ref}| \leq e^V \quad \forall i = 1, \dots, n$$
$$\lim_{t\to\infty} |\omega_i(t) - \omega^{ref}| \leq e^\omega \quad \forall i = 1, \dots, n,$$

where V_i^{ref} is the reference DC voltage of converter i, ω^{ref} is the reference frequency and e^V and e^ω are given scalars.

Remark 1. *It is in general not possible to have $e^V = 0$, since this does not allow for the currents in the HVDC grid to change. The bounds e^{gen} and e^ω on the other hand, can in theory be zero. However, this may be hard to achieve with limited communication.*

IV. Decentralized MTDC control

In this section we summarize previous results on decentralized control of MTDC systems. The detailed results and proofs can be found in [2]. We consider the following decentralized frequency droop controllers for the control of the AC systems connected through an MTDC network

$$P_i^{\text{gen}} = -K_i^{\text{droop}}(\omega_i - \omega^{\text{ref}}), \tag{3}$$

where ω_i is the frequency of the generator, ω^{ref} is the reference frequency (e.g., 50 or 60 Hz), and $K_i^{\text{droop}} > 0$. The local controllers governing the power injections into the MTDC network are given by

$$P_i^{\text{inj}} = P_i^{\text{inj, nom}} + K_i^\omega(\omega_i - \omega^{\text{ref}}) + K_i^V(V_i^{\text{ref}} - V_i), \tag{4}$$

where $P_i^{\text{inj, nom}}$ is the nominal injected power, and $K_i^\omega > 0$ and $K_i^V > 0$ are positive controller gains for all $i = 1, \dots, n$. The HVDC converter is assumed to be perfect and instantaneous, i.e., injected power on the AC side is immediately converted to DC power without losses. Furthermore the dynamics of the converter are ignored, implying that the converter tracks the output of controller (4) perfectly. This assumption is reasonable due to the dynamics of the converter typically being orders of magnitudes faster than the AC dynamics [11]. The relation between the injected HVDC current and the injected AC power is thus given by

$$V_i I_i^{\text{inj}} = P_i^{\text{inj}}. \tag{5}$$

By assuming $V_i = V^{\text{nom}}\ \forall i = 1, \dots, n$, we obtain

$$V^{\text{nom}} I_i^{\text{inj}} = P_i^{\text{inj}}. \tag{6}$$

Furthermore, we assume that the nominal generated power equals to the nominal injected power.

Assumption 1. $P_i^{nom} = P_i^{inj,\ nom}\ \forall i = 1, \dots, n.$

Theorem 1. *The equilibrium of the decentralized MTDC control system with dynamics given by* (1)*,* (2)*,* (3)*,* (4)*, and where* (6) *holds, is globally asymptotically stable [2].*

We will now study the asymptotic voltages and frequencies as well as the generated power of the MTDC system. We make the following assumption on the controller gains.

Assumption 2. *The controller gains satisfy* $K_i^\omega = k^\omega, K_i^{droop} = k^{droop}, K_i^V = k^V\ \forall i = 1, \dots, n.$

Theorem 2. *Given that Assumption 2 holds, then for the HVDC and AC systems* (1)*,* (2) *with generation control* (3) *and converter control* (4) *and where* (6) *holds, Objective 1 is satisfied for* $e^{gen} = e_{dec}^{gen}$*,* $e^V = e_{dec}^V$ *and* $e^\omega = e_{dec}^\omega$ *[2], where*

$$e_{dec}^{gen} = \frac{k^{droop} \max_i P_i^m}{k^{droop} + k^\omega} \left((n-1) + \frac{k^V}{V^{nom}} \sum_{i=2}^{n} \frac{1}{\lambda_i(\mathcal{L}_R)} \right)$$

$$e_{dec}^V = \frac{k^\omega}{n k^{droop} k^V} \left| \sum_{i=1}^{n} P_i^m \right| + \frac{k^\omega \max_i \left| P_i^m \right|}{(k^\omega + k^{droop}) V^{nom}} \sum_{i=2}^{n} \frac{1}{\lambda_i(\mathcal{L}_R)}$$

$$e_{dec}^\omega = \frac{1}{n k^{droop}} \left| \sum_{i=1}^{n} P_i^m \right| + \frac{\max_i P_i^m}{k^{droop} + k^\omega} \left((n-1) + \frac{k^V}{V^{nom}} \sum_{i=2}^{n} \frac{1}{\lambda_i(\mathcal{L}_R)} \right).$$

In the following section we will show that the above upper bounds can be tightened by a secondary control layer.

V. Distributed secondary frequency control

In this section we study a distributed secondary frequency controller to tighten the stationary error bounds of the closed-loop system given in Theorem 2. To implement a distributed controller, we assume the existence of a communication, enabling communication between all AC generators. We will consider two distributed secondary controllers; a controller where any pair of generators can communicate directly, and a controller where only neighbouring generators can communicate directly. These two controllers correspond require a complete communication graph and a communication graph containing a spanning tree, respectively. The corresponding topologies of these controllers are illustrated in Figure 1. The first generation controller of the AC systems is given by

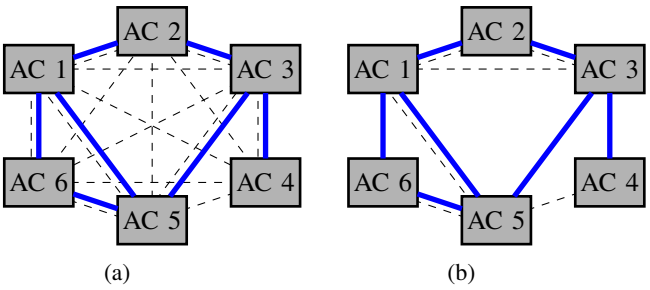

(a) (b)

Figure 1: Illustration of the HVDC grid and the communication network topologies. The HVDC lines are illustrated with solid lines, while comminication lineas are illustrated with dashed lines. (a) shows the structure of the complete communication structure of (7), while (b) shows the structure of the communication structure of (8).

$$P_i^{\text{gen}} = -K_i^{\text{droop}}(\omega_i - \omega^{\text{ref}}) - \frac{K_i^V}{K_i^\omega} K_i^{\text{droop, I}} \frac{1}{n} \sum_{i=1}^{n} \eta_i$$
$$\dot{\eta}_i = K_i^{\text{droop,I}}(\omega_i - \omega^{\text{ref}}) - \gamma \eta_i, \tag{7}$$

where $\gamma, K_i^{\text{droop, I}},\ i = 1, \dots, n$ are positive constants. If $\gamma = 0$, then η_i becomes a scaled integral state of the local frequency deviation $(\omega_i - \omega^{\text{ref}})$. The second generation controller of the AC systems is given by

$$P_i^{\text{gen}} = -K_i^{\text{droop}}(\omega_i - \omega^{\text{ref}}) - \frac{K_i^V}{K_i^\omega} K_i^{\text{droop, I}} \eta_i$$
$$\dot{\eta}_i = K_i^{\text{droop,I}}(\omega_i - \omega^{\text{ref}}) - \delta \sum_{j \in \mathcal{N}_i} c_{ij}(\eta_i - \eta_j). \tag{8}$$

We assume $c_{ij} = c_{ji}$, i.e., the communication graph is undirected. The above controller can be interpreted as a distributed PI-controller, with a distributed consensus filter acting on the integral states η_i. In contrast to the controller (7), (8) does not rely on a complete communication graph. Note that we make no assumption that the communication topology resembles the topology of the MTDC system.

A. Stability analysis

Combining the voltage dynamics (1), the frequency dynamics (2) and the generation control (7) or (8), the converter controller (4) and the power-current relationship (6), together with Assumption 1 and defining $\hat{\omega} = \omega - \omega^{\text{ref}} 1_n$ and $\hat{V} = V - V^{\text{ref}}$, where $V^{\text{ref}} = [V_1^{\text{ref}}, \dots, V_n^{\text{ref}}]$, we obtain the closed-loop dynamics given by (9) or (11), respectively, where $\eta = [\eta_1, \dots, \eta_n]^T$, $K^{\text{droop,I}} = \text{diag}([K_1^{\text{droop,I}}, \dots, K_n^{\text{droop,I}}])$, and $\mathcal{L}_c$ is the weighted Laplacian matrix of the communication graph with edge-weights c_{ij}. The details of the derivations have been omitted, but the derivation follows the steps taken

$$\begin{bmatrix}\dot{\hat{\omega}}\\ \dot{\hat{V}}\\ \dot{\eta}\end{bmatrix}=\begin{bmatrix}-M(K^{\omega}+K^{\text{droop}}) & MK^{V} & -\frac{1}{n}MK^{V}(K^{\omega})^{-1}K^{\text{droop,I}}1_{n\times n}\\ \frac{1}{V^{\text{nom}}}EK^{\omega} & -E\left(\mathcal{L}_R+\frac{K^{V}}{V^{\text{nom}}}\right) & 0_{n\times n}\\ K^{\text{droop,I}} & 0_{n\times n} & -\gamma I_n\end{bmatrix}\begin{bmatrix}\hat{\omega}\\ \hat{V}\\ \eta\end{bmatrix}+\begin{bmatrix}MP^{m}\\ 0_{n\times 1}\\ 0_{n\times 1}\end{bmatrix} \tag{9}$$

$$\begin{bmatrix}\dot{\hat{\omega}}\\ \dot{\hat{V}}\\ \dot{\eta}'\end{bmatrix}=\begin{bmatrix}-M(K^{\omega}+K^{\text{droop}}) & MK^{V} & -MK^{V}(K^{\omega})^{-1}K^{\text{droop,I}}1_{n}\\ \frac{1}{V^{\text{nom}}}EK^{\omega} & -E\left(\mathcal{L}_R+\frac{K^{V}}{V^{\text{nom}}}\right) & 0_{n}\\ \frac{1}{n}1_n^{T}K^{\text{droop,I}} & 0_n^{T} & -\gamma\end{bmatrix}\begin{bmatrix}\hat{\omega}\\ \hat{V}\\ \eta'\end{bmatrix}+\begin{bmatrix}MP^{m}\\ 0_{n\times 1}\\ 0\end{bmatrix} \tag{10}$$

$$\begin{bmatrix}\dot{\hat{\omega}}\\ \dot{\hat{V}}\\ \dot{\eta}\end{bmatrix}=\begin{bmatrix}-M(K^{\omega}+K^{\text{droop}}) & MK^{V} & -MK^{V}(K^{\omega})^{-1}K^{\text{droop,I}}\\ \frac{1}{V^{\text{nom}}}EK^{\omega} & -E\left(\mathcal{L}_R+\frac{K^{V}}{V^{\text{nom}}}\right) & 0_{n\times n}\\ K^{\text{droop,I}} & 0_{n\times n} & -\delta\mathcal{L}_c\end{bmatrix}\begin{bmatrix}\hat{\omega}\\ \hat{V}\\ \eta\end{bmatrix}+\begin{bmatrix}MP^{m}\\ 0_{n\times 1}\\ 0_{n\times 1}\end{bmatrix} \tag{11}$$

in Section IV in [2]. Clearly the representation (9) is not minimal with respect to the output $y=[\hat{\omega}^T,\hat{V}^T]^T$, since the integral states η are redundant. It is easily shown that substituting the projection

$$\eta'=\frac{1}{n}1_n^{T}\eta, \tag{12}$$

in (9), the output dynamics remain unchanged. Even though the dynamics (9) are redundant, they show that the secondary control layer can be implemented distributively. Each AC generator needs only to compute its local integral state, and communicate this to the remaining generators. In order to prove stability of the closed-loop system, it is however essential to consider the reduced system after applying the projection (12), which is given by (10). This system can be interpreted as a centralized implementation of (9), where the single integral state η' is computed centrally with access to all frequency measurements. By decomposing (10) and (11) into two subsystems, we obtain

$$\begin{cases}\dot{\hat{\omega}}=-M(K^{\text{droop}}+K^{\omega})\hat{\omega}\\ \qquad -\frac{1}{n}MK^{V}(K^{\omega})^{-1}K^{\text{droop,I}}1_n\eta'+MK^{V}u_1\\ \dot{\eta}'=\frac{1}{n}1_n^{T}K^{\text{droop,I}}\hat{\omega}-\gamma\eta'\\ y_1=\frac{1}{V^{\text{nom}}}K^{\omega}\hat{\omega}\end{cases} \tag{S_1'}$$

$$\begin{cases}\dot{\hat{\omega}}=-M(K^{\text{droop}}+K^{\omega})\hat{\omega}\\ \qquad -\frac{1}{n}MK^{V}(K^{\omega})^{-1}K^{\text{droop,I}}\eta+MK^{V}u_1\\ \dot{\eta}=1_n^{T}K^{\text{droop,I}}\hat{\omega}-\delta\mathcal{L}_c\eta\\ y_1=\frac{1}{V^{\text{nom}}}K^{\omega}\hat{\omega}\end{cases} \tag{$\hat{S}_1'$}$$

$$\begin{cases}\dot{\hat{V}}=-E\left(\mathcal{L}_R+1/V^{\text{nom}}K^{V}\right)\hat{V}+Eu_2\\ y_2=\hat{V},\end{cases} \tag{S_2}$$

where (S_1') and $(\hat{S}_1')$ are interconnected with (S_2) through $u_1=y_2+(K^{V})^{-1}P^{m}, u_2=y_1$. Before proceeding with the main stability results, we recall the definitions of passivity and zero-state observability. Consider a system

$$\begin{aligned}\dot{x}&=f(x,u)\\ y&=h(x,u).\end{aligned} \tag{13}$$

Definition 1. *The system* (13) *is said to be* strictly passive *if there exists a p.s.d. function $W(x)$, and a p.d. function $\psi(x)$ such that $u^Ty\geq\dot{W}+\psi(x)$. The same system is said to be* output strictly passive *if there exists a p.s.d. function $W(x)$, and some function $\rho(y)$ such that $u^Ty\geq\dot{W}+y^T\rho(y)$, and $y^T\rho(y)>0$ for $y\neq 0$ [20], [10].*

Definition 2. *The system* (13) *is said to be* zero-state observable *if no solution of $\dot{x}=f(x,0)$ can stay identically on $S=\{h(x,0)=0\}$, other than the zero solution $x(0)\equiv 0$.*

Proposition 1. *The system (S_1') is strictly passive if $\gamma>0$, output strictly passive and zero-state observable if $\gamma=0$.*

Proof. Consider the storage function $W_1'=\frac{1}{2V^{\text{nom}}}\left(\hat{\omega}^TK^{\omega}(K^{V})^{-1}M^{-1}\hat{\omega}+\eta'^2\right)$. Differentiating W_1' with respect to time along trajectories of (S_1') yields

$$\begin{aligned}\dot{W}_1'&=\frac{1}{V^{\text{nom}}}\left(\hat{\omega}^T\left(K^{\omega}(K^{V})^{-1}M^{-1}\right)\dot{\hat{\omega}}+\eta^T\dot{\eta}\right)\\ &=\frac{1}{V^{\text{nom}}}\Big(-\hat{\omega}^TK^{\omega}(K^{V})^{-1}(K^{\text{droop}}+K^{\omega})\hat{\omega}\\ &\quad-\frac{1}{n}\hat{\omega}^TK^{\text{droop, I}}1_n\eta'+\hat{\omega}^TK^{\omega}u_1\\ &\quad+\eta'\Big(\frac{1}{n}1_n^{T}K^{\text{droop,I}}\hat{\omega}-\gamma\eta'\Big)\Big)\\ &=-\frac{1}{V^{\text{nom}}}\hat{\omega}^TK^{\omega}(K^{V})^{-1}(K^{\text{droop}}+K^{\omega})\hat{\omega}\\ &\quad-\gamma\eta'^2+y_1^Tu_1,\end{aligned}$$

which shows that (S_1') is strictly passive for $\gamma>0$, and output strictly passive if $\gamma=0$. It is easily verified that (S_1') is zero-state observable. □

Proposition 2. *The system $(\hat{S}_1')$ is output strictly passive and zero-state observable for $\delta>0$.*

Proof. Consider the storage function

$$W_1' = \frac{1}{2V^{\text{nom}}}\left(\hat{\omega}^T K^\omega (K^V)^{-1} M^{-1}\hat{\omega} + \eta^T\eta\right).$$

Differentiating W_1' along trajectories of (S_1') yields

$$\begin{aligned}\dot{W}_1' &= \frac{1}{V^{\text{nom}}}\left(\hat{\omega}^T\left(K^\omega(K^V)^{-1}M^{-1}\right)\dot{\hat{\omega}} + \eta'\dot{\eta}'\right)\\ &= \frac{1}{V^{\text{nom}}}\Big(-\hat{\omega}^T K^\omega (K^V)^{-1}(K^{\text{droop}}+K^\omega)\hat{\omega}\\ &\quad - \hat{\omega}^T K^{\text{droop, I}}\eta + \hat{\omega}^T K^\omega u_1\\ &\quad + \eta^T\left(K^{\text{droop,I}}\hat{\omega} - \delta\mathcal{L}_c\eta\right)\Big)\\ &= -\frac{1}{V^{\text{nom}}}\hat{\omega}^T K^\omega (K^V)^{-1}(K^{\text{droop}}+K^\omega)\hat{\omega}\\ &\quad - \delta\eta^T\mathcal{L}_c\eta + y_1^T u_1,\end{aligned}$$

which shows that $(\hat{S}_1')$ is output strictly passive. It is easily verified that (S_1') is zero-state observable. □

Lemma 1. *The system* (S_2) *is strictly passive [2].*

Theorem 3. *The equilibria of the systems defined by* (10) *and* (11) *are globally asymptotically stable.*

Proof. The equilibrium of the interconnection of any two strictly passive systems is asymptotically stable [10]. Since the storage functions are radially unbounded, stability is global. □

B. Equilibrium analysis

In this section we study the properties of the equilibria of (10) and (11), respectively. We show that by employing the aforementioned secondary frequency control schemes, it is possible to tighten the error bounds in Theorem 2. Analogous to Section IV, we assume uniform controller gains.

Theorem 4. *Assume that Assumptions 1 and 2 hold, mutatis mutandis. Consider the HVDC and AC systems* (1)*,* (2) *with generation control* (3) *and where the relation* (6) *holds. Objective 1 is satisfied for the secondary controller* (7) *when* $\gamma \to 0^+$*, and for the secondary controller* (8) *when* $\delta \to +\infty$*. In both cases, Objective 1 is satisfied for* $e^{dist} = e^{gen}_{dist}$*,* $e^V = e^V_{dec}$ *and* $e^\omega = e^\omega_{dist}$*, where*

$$\begin{aligned}e^{gen}_{dist} &= \frac{k^{droop}\max_i P_i^m}{k^{droop}+k^\omega}\left((n-1)+\frac{k^V}{V^{nom}}\sum_{i=2}^n\frac{1}{\lambda_i(\mathcal{L}_R)}\right)\\ e^V_{dist} &= \frac{k^\omega\max_i\left|P_i^m\right|}{(k^{droop}+k^\omega)V^{nom}}\sum_{i=2}^n\frac{1}{\lambda_i(\mathcal{L}_R)}\\ e^\omega_{dist} &= \frac{\max_i P_i^m}{k^{droop}+k^\omega}\left((n-1)+\frac{k^V}{V^{nom}}\sum_{i=2}^n\frac{1}{\lambda_i(\mathcal{L}_R)}\right).\end{aligned}$$

Furthermore $1_n^T\hat{\omega} = 1_n^T\hat{V} = 0$*, i.e., the average frequency and voltage deviations are zero.*

Proof. Before studying the equilibria of (10) and (11), we will show that under the assumptions that $\gamma \to 0^+$, and $\delta \to +\infty$, the first $2n$ rows of the equilibria of (10) and (11) are identical. Consider the last row of the equilibrium of (10), which as $\gamma \to 0$ implies $1_n^T\hat{\omega} = 0$. Thus, premultiplying the $(n+1)$th to $2n$th rows of the equilibrium of (10) with $1_n^T C$ yields $1_n^T\hat{V} = 0$. Finally, premultiplying the first n rows of (10) with $1_n^T M^{-1}$ yields

$$\frac{nk^V k^{\text{droop, I}}}{k^\omega}\eta' = -1_n^T P^m. \tag{14}$$

Now consider the equilibrium of (11). Following similar steps as in the manipulation of (10), we obtain that $1_n^T\hat{\omega} = 0$ and $1_n^T\hat{V} = 0$. Thus premultiplying the first n rows of the equilibrium of (11) with $1_n^T M^{-1}$, we obtain

$$\frac{k^V k^{\text{droop, I}}}{k^\omega}1_n^T\eta = -1_n^T P^m. \tag{15}$$

We write η as a linear combination $\eta = \sum_{i=1}^n a_i^0 v_i^0$, where v_i^0 is the (normed) ith eigenvector of $\mathcal{L}_c$. Inserting the eigen decomposition of η in (15) yields

$$a_i^0 = -\frac{1_n^T I^{\text{inj}} k^\omega\sqrt{n}}{k^V k^{\text{droop, I}}},$$

since $v_1^0 = \frac{1}{\sqrt{n}}1_n$. In order to determine a_i^0 for $i \geq 2$, we consider the last n rows of the equilibrium of (11). Again, using the eigen decomposition of η we obtain

$$k^{\text{droop, I}}\hat{\omega} = \delta\mathcal{L}_c\sum_{i=1}^n a_i^0 v_i^0 = \sum_{i=2}^n a_i^0\lambda_i^0 v_i^0.$$

Premultiplying the above equation with $(v_j^0)^T$ we obtain

$$a_j^0 = \frac{k^{\text{droop, I}}(v_j^0)^T\hat{\omega}}{\delta\lambda_j^0}.$$

Clearly $a_j^0 \to 0$ as $\delta \to \infty$ for $j = 2,\ldots,n$, if $\hat{\omega}$ is bounded. But $\hat{\omega}$ must be bounded since the system matrix of (11) is full rank, implying that the steady-state solution to (11) is bounded. Thus, at steady-state we have $\eta_i = \eta^*\ \forall i = 1,\ldots,n$. Inserting this in (15) yields

$$\frac{nk^V k^{\text{droop, I}}}{k^\omega}\eta^* = -1_n^T P^m. \tag{16}$$

Comparing (16) with (14), it is clear that the first $2n$ rows of the equilibria of (10) and (11) are identical, and thus define the same solutions. We thus proceed only considering the equilibrium of (10), whose last row implies

$$\eta' = \frac{k^{\text{droop, I}}}{n\gamma}1_n^T\hat{\omega}. \tag{17}$$

Eliminating η' in (10), we obtain

$$\begin{bmatrix}-(k^\omega+k^{\text{droop}})I_n - \frac{k^V(k^{\text{droop, I}})^2}{n\gamma k^\omega}1_{n\times n} & k^V I_n\\ \frac{k^\omega}{V^{\text{nom}}}I_n & -(\mathcal{L}_R+\frac{k^V}{V^{\text{nom}}}I_n)\end{bmatrix}\begin{bmatrix}\hat{\omega}\\ \hat{V}\end{bmatrix} = \begin{bmatrix}-P^m\\ 0_{n\times 1}\\ 0\end{bmatrix}. \tag{18}$$

Premultiplying the last n rows of (18) with $\frac{V^{\text{nom}}}{k^\omega}\left((k^\omega+k^{\text{droop}})I_n + \frac{k^V(k^{\text{droop, I}})^2}{n\gamma k^\omega}1_{n\times n}\right)$ and adding to

the first n yields

$$\left(-k^V I_n + \frac{V^{\text{nom}}}{k^\omega} \left((k^\omega + k^{\text{droop}}) I_n + \frac{k^V (k^{\text{droop, I}})^2}{n\gamma k^\omega} 1_{n\times n} \right) \times \left(\mathcal{L}_R + \frac{k^V}{V^{\text{nom}}} I_n \right) \right) \hat{V} = P^m,$$

which after some simplification gives

$$\left(\frac{k^V}{k^\omega} \left(k^{\text{droop}} I_n + \frac{k^V (k^{\text{droop, I}})^2}{n\gamma k^\omega} 1_{n\times n} \right) + \frac{V^{\text{nom}}}{k^\omega} \left(k^\omega + k^{\text{droop}} \right) \mathcal{L}_R \right) \hat{V} \triangleq A_1 \hat{V} = P^m. \quad (19)$$

Write $\hat{V} = \sum_{i=1}^n a_i^1 v_i^1$, where v_i^1 is an eigenvector of A_1 with the corresponding eigenvalue λ_i^1. It is easily verified that $\frac{1}{\sqrt{n}} 1_n$ is an eigenvalue of A_1, which we denote v_1^1. Since A_1 is symmetric, its eigenvectors can be chosen to form an orthonormal basis. By premultiplying (19) with $(v_j^1)^T$, and keeping in mind that $A_1 v_j^1 = \lambda_j^1 v_j^1$, we obtain $a_j = (v_j^1)^T P^m / \lambda_j^1$. By direct computation we obtain

$$\lambda_1^1 = \frac{k^V}{k^\omega} \left((k^{\text{droop}}) + \frac{k^V (k^{\text{droop, I}})^2}{\gamma k^\omega} \right),$$

by which we conclude that $\lambda_1^1 \to \infty$ as $\gamma \to 0^+$. Thus $a_1 \to 0$ as $\gamma \to 0^+$. For $i \geq 2$ we obtain after some calculations $\lambda_i^1 \geq \frac{V^{\text{nom}}}{k^\omega} \left(k^\omega + k^{\text{droop}} \right) \lambda_i(\mathcal{L}_R)$. Thus, we obtain the following bound on $\hat{V}$:

$$\begin{aligned} \lim_{\gamma\to 0} \left\| \hat{V} \right\|_\infty &= \left\| \sum_{i=2}^n \frac{(v_i^1)^T P^m}{\lambda_i} v_i^1 \right\|_\infty \\ &\leq \frac{k^\omega \max_i \left| P_i^m \right|}{(k^\omega + k^{\text{droop}}) V^{\text{nom}}} \sum_{i=2}^n \frac{1}{\lambda_i^1(\mathcal{L}_R)}. \end{aligned}$$

Premultiplying the first n rows of (18) with $\frac{1}{k^V}(\mathcal{L}_R + \frac{k^V}{V^{\text{nom}}} I_n)$, and adding to the last n rows of (18) yields

$$\begin{aligned} &\left(-\frac{k^\omega}{V^{\text{nom}}} I_n + \frac{1}{k^V} \left(\mathcal{L}_R + \frac{k^V}{V^{\text{nom}}} I_n \right) \right. \\ &\quad \left. \times \left((k^\omega + k^{\text{droop}}) I_n + \frac{k^V (k^{\text{droop, I}})^2}{n\gamma k^\omega} 1_{n\times n} \right) \right) \hat{\omega} \\ &= \frac{1}{k^V} \left(\mathcal{L}_R + \frac{k^V}{V^{\text{nom}}} I_n \right) P^m. \end{aligned}$$

After some algebra, the following expression is obtained

$$\begin{aligned} &\left(\frac{k^{\text{droop}}}{V^{\text{nom}}} I_n + \frac{k^V (k^{\text{droop}})^2}{V^{\text{nom}} k^\omega n\gamma} 1_{n\times n} + \frac{k^{\text{droop}} + k^\omega}{k^V} \mathcal{L}_R \right) \hat{\omega} \\ &\triangleq A_2 \hat{\omega} = \frac{1}{k^V} \left(\mathcal{L}_R + \frac{k^V}{V^{\text{nom}}} I_n \right) P^m. \end{aligned} \quad (20)$$

Again, write $\hat{\omega} = \sum_{i=1}^n a_i^2 v_i^2$, where v_i^2 is the eigenvector of A_2 with eigenvalue λ_i^2. Let λ_1^2 denote the eigenvalue of A_2 with eigenvector $\frac{1}{\sqrt{n}} 1_n$. By direct computation

$$\lambda_1^2 = \frac{k^{\text{droop}}}{V^{\text{nom}}} + \frac{k^V (k^{\text{droop,I}})^2}{V^{\text{nom}} k^\omega \gamma},$$

and clearly $\lambda_1^2 \to \infty$ as $\gamma \to 0^+$, implying that $a_1^2 \to 0$ as $\gamma \to 0^+$. For the remaining eigenvalues, i.e., $i \geq 2$, we obtain after some calculations

$$\lambda_i^2 \geq \frac{k^{\text{droop}} + k^\omega}{k^V} \lambda_i(\mathcal{L}_R).$$

By premultiplying (20) with $(a_j^2)^T$, we obtain

$$a_j^2 = \frac{(v_j^2)^T \left(\mathcal{L}_R + \frac{k^V}{V^{\text{nom}}} I_n \right) P^m}{k^V \lambda_j^2}.$$

Thus we obtain the following bound on $\hat{\omega}$

$$\begin{aligned} \lim_{\gamma\to 0} \|\hat{\omega}\|_\infty &= \left\| \sum_{i=2}^n \frac{(v_i^2)^T \left(\mathcal{L}_R + \frac{k^V}{V^{\text{nom}}} I_n \right) P^m}{k^V \lambda_i^2} v_i^2 \right\|_\infty \\ &\leq \sum_{i=2}^n \left\| \frac{\left(\lambda_i(\mathcal{L}_R) + \frac{k^V}{V^{\text{nom}}} \right) (v_i^2)^T P^m}{(k^{\text{droop}} + k^\omega) \lambda_i(\mathcal{L}_R)} v_i^2 \right\|_\infty \\ &\leq \frac{\max_i P_i^m}{k^{\text{droop}} + k^\omega} \left((n-1) + \frac{k^V}{V^{\text{nom}}} \sum_{i=2}^n \frac{1}{\lambda_i(\mathcal{L}_R)} \right), \end{aligned}$$

where we have used the fact that the eigenvectors of A_2 are also eigenvectors of $\mathcal{L}_R$. Finally, we consider the power output of the generation control. Note that $\lim_{\gamma\to 0} \lambda_1^2 = \frac{k^V (k^{\text{droop,I}})^2}{V^{\text{nom}} k^\omega \gamma}$. Thus, when $\gamma \to 0$, we have by (17) that

$$\begin{aligned} \lim_{\gamma\to 0} P^{\text{gen}} &= -k^{\text{droop}} \hat{\omega} - \frac{k^V k^{\text{droop,I}}}{n k^\omega} 1_n \eta' \\ &= -\left(k^{\text{droop}} I_n + \frac{k^V (k^{\text{droop,I}})^2}{n^2 \gamma k^\omega} 1_{n\times n} \right) \hat{\omega} \\ &= -\left(k^{\text{droop}} I_n + \frac{k^V (k^{\text{droop,I}})^2}{n^2 \gamma k^\omega} 1_{n\times n} \right) \sum_{i=1}^n a_i^2 v_i^2 \\ &= -\left(k^{\text{droop}} I_n + \frac{k^V (k^{\text{droop,I}})^2}{n^2 \gamma k^\omega} 1_{n\times n} \right) \\ &\quad \times \left(\frac{\gamma k^\omega 1_n^T P^m}{n k^V (k^{\text{droop,I}})^2} 1_n \right. \\ &\quad \left. + \sum_{i=2}^n \frac{(v_i^2)^T \left(\mathcal{L}_R + \frac{k^V}{V^{\text{nom}}} I_n \right) P^m}{k^V \lambda_i^2} v_i^2 \right). \end{aligned}$$

Noting that $v_1^2 = \frac{1}{\sqrt{n}}$, we have that $1_n^T v_i^2 = 0$ for $i \geq 2$. By letting $\gamma \to 0$, the above equation simplifies to

$$\begin{aligned} \lim_{\gamma\to 0} P^{\text{gen}} &= -\frac{1}{n} 1_n^T P^m 1_n \\ &\quad - \sum_{i=2}^n \frac{k^{\text{droop}} (v_i^2)^T \left(\mathcal{L}_R + \frac{k^V}{V^{\text{nom}}} I_n \right) P^m}{k^V \lambda_i^2} v_i^2. \end{aligned}$$

Using the previously derived lower bound on λ_i^2 for $i \geq 2$, we obtain the following bound on the generated power

$$\begin{aligned}
&\left\| \frac{1}{n} 1_n^T P^m 1_n + P^{\text{gen}} \right\|_\infty \\
&= \left\| \sum_{i=2}^{n} \frac{k^{\text{droop}} (v_i^2)^T \left(\mathcal{L}_R + \frac{k^V}{V^{\text{nom}}} I_n \right) P^m}{k^V \lambda_i^2} v_i^2 \right\|_\infty \\
&\leq \sum_{i=2}^{n} \left\| \frac{k^{\text{droop}} k^V \left(\lambda_i(\mathcal{L}_R) + \frac{k^V}{V^{\text{nom}}} \right) (v_i^2)^T P^m}{k^V (k^{\text{droop}} + k^\omega) \lambda_i(\mathcal{L}_R)} v_i^2 \right\|_\infty \\
&\leq \frac{k^{\text{droop}} \max_i P_i^m}{k^{\text{droop}} + k^\omega} \left((n-1) + \frac{k^V}{V^{\text{nom}}} \sum_{i=2}^{n} \frac{1}{\lambda_i(\mathcal{L}_R)} \right) \quad \square
\end{aligned}$$

Remark 2. *The upper bounds on the AC frequency and the DC voltage errors, i.e., e^ω and e^V in Theorem 4 are lower than the corresponding bounds in Theorem 2 given the same network and controller parameters. In particular*

$$e^V_{dec} - e^V_{dist} = \frac{k^\omega}{n k^{droop} k^V} \left| \sum_{i=1}^{n} P_i^m \right|$$

$$e^\omega_{dec} - e^\omega_{dist} = \frac{1}{n k^{droop}} \left| \sum_{i=1}^{n} P_i^m \right|.$$

However, as the bounds are conservative, no conclusion about the actual control errors can be drawn.

VI. Simulations

In this section, simulations are conducted on a test system to validate the performance of the proposed controllers. The simulation was performed in Matlab, using a dynamic phasor approach based on [8] The test system is illustrated in Figure 2. The parameters of the MTDC grid are given in I, and are chosen uniformly for all VSC stations. Note that we in the simulation also consider the inductances L_{ij} and capacitances C_{ij} of the HVDC lines. The capacitances of the terminals are assumed to be given by $C_i = 0.375 \times 10^{-3}$ p.u. The AC grid parameters were obtained from [15]. The generators are modeled as a 6^th order machine model controlled by an automatic voltage controller and a governor [11]. The loads in the grid are assumed to be equipped with an ideal power controller. The controllers (3), (7) and (8)

Table I: HVDC grid line parameters

i	j	R_{ij} [p.u.]	L_{ij} [10^{-3} p.u.]	C_{ij} [p.u.]
1	2	0.0586	0.2560	0.0085
1	3	0.0586	0.2560	0.0085
2	3	0.0878	0.3840	0.0127
2	4	0.0586	0.2560	0.0085
2	5	0.0732	0.3200	0.0106
2	6	0.1464	0.6400	0.0212
3	4	0.0586	0.2560	0.0085
3	5	0.1464	0.6400	0.0212
4	5	0.0732	0.3200	0.0106
5	6	0.1464	0.6400	0.0212

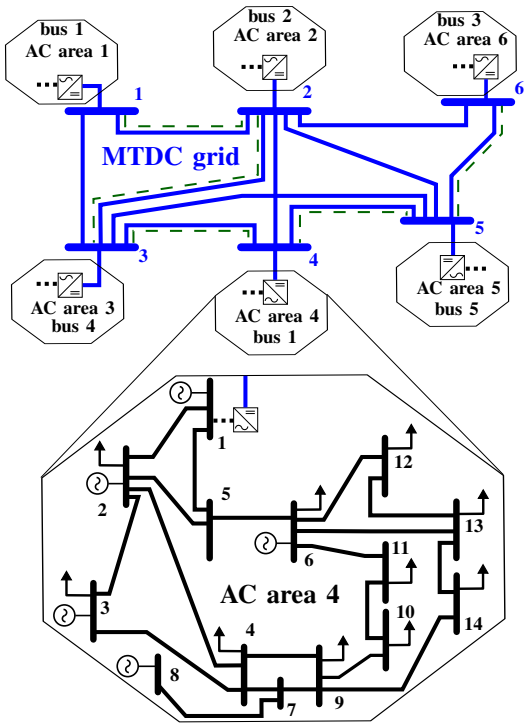

Figure 2: MTDC test system, consisting of a 6-terminal MTDC grid. Each terminal is connected to an IEEE 14 bus AC grid, sketched as octagons. The dashed lines illustrate the topology of the communication grid of the controller (8).

Table II: Controller Parameter

K_i^ω	K_i^V	K_i^{droop}	$K_i^{\text{droop, I}}$	γ	δ
9000	110	8	10	0	5

were applied to the aforementioned test grid. At time $t = 1$ the output of one generator in area 1 was reduced by 0.2 p.u., simulating a fault. The communication network of controller (8) is illustrated by the dashed lines in Figure 2. Figure 3 shows the frequency response of all AC grids for the three controllers considered. Figure 4 shows the DC voltages of the terminals. Figure 5 shows the total change in the generated power within each AC area. It can be noted that immediately after the fault, the frequency at the corresponding AC area drops. The frequency drop is followed by a voltage drop in all terminals, and a frequency drop at all AC areas. The frequencies and voltages converge to new stationary values after approximately 30 s. We note that the asymptotic error of the frequencies and voltages are significantly smaller when the controllers (7) and (8) are employed, than when the decentralized droop controller (3) is employed. The generated power is shared fairly between the AC areas.

VII. Discussion and Conclusions

In this paper we have studied controllers for sharing primary and secondary frequency control reserves in asynchronous AC systems connected through an MTDC system. We have reviewed a decentralized droop controller, and

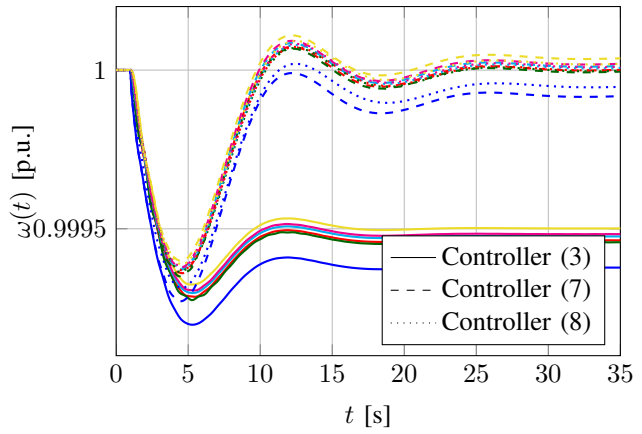

Figure 3: Average frequencies in the AC areas for the controllers (3), (7) and (8), respectively.

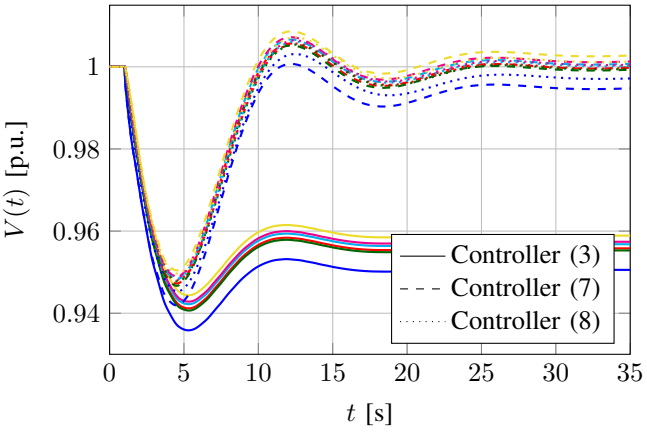

Figure 4: DC terminal voltages for the controllers (3), (7) and (8), respectively.

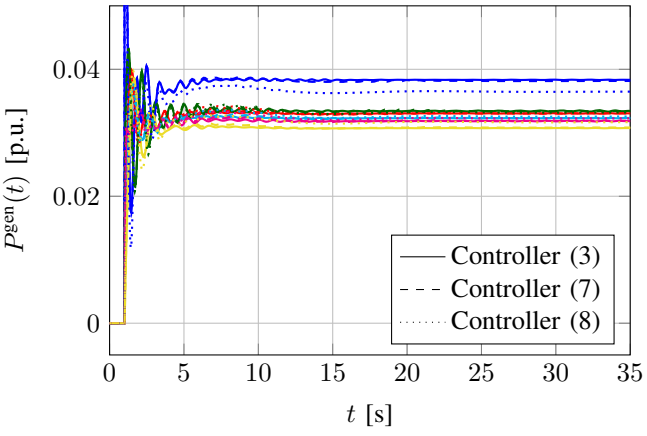

Figure 5: Total generated power in the AC areas for the controllers (3), (7) and (8), respectively.

later expanded this to two distributed secondary frequency controllers. The distributed controllers use both local and neighboring frequency measurements of the AC grids, as well as the local DC voltage measurements. The resulting equilibria of the closed-loop system was shown to be globally asymptotically stable by using passivity arguments. We also showed bounds for the asymptotic deviations of the DC voltages and the AC frequencies from their reference values. The obtained bounds are lower than the corresponding bounds when using only decentralized droop control. Furthermore the generated power from the primary frequency control is approximately shared fairly between the AC areas, and the error from fair power sharing is bounded. We have furthermore demonstrated our results on a 6 terminal MTDC system with connected AC systems. Future work will focus on eliminating the static errors in the frequencies.

References

[1] M. Andreasson, D. V. Dimarogonas, and K. H. Johansson. Distributed controllers for multi-terminal HVDC transmission systems. *arXiv preprint:1411.1864*, 2014.

[2] M. Andreasson, R. Wiget, D. V. Dimarogonas, K. H. Johansson, and G. Andersson. Distributed primary frequency control through multi-terminal HVDC transmission systems. 2015.

[3] U. Axelsson, A. Holm, C. Liljegren, M. Aberg, K. Eriksson, and O. Tollerz. The Gotland HVDC light project-experiences from trial and commercial operation. In *Electricity Distribution, 2001. Part 1: Contributions. CIRED. 16th International Conference and Exhibition on (IEE Conf. Publ No. 482)*, volume 1, pages 5–pp. IET, 2001.

[4] P. Bresesti, W.L. Kling, R.L. Hendriks, and R. Vailati. HVDC connection of offshore wind farms to the transmission system. *IEEE Transactions on Energy Conversion*, 22(1):37–43, 2007.

[5] J. Dai and G. Damm. An improved control law using HVDC systems for frequency control. In *Power systems computation conference*, 2011.

[6] J. Dai, Y. Phulpin, A. Sarlette, and D. Ernst. Impact of delays on a consensus-based primary frequency control scheme for AC systems connected by a multi-terminal HVDC grid. In *IEEE Bulk Power System Dynamics and Control*, pages 1–9, 2010.

[7] J. Dai, Y. Phulpin, A. Sarlette, and D. Ernst. Voltage control in an HVDC system to share primary frequency reserves between non-synchronous areas. In *Power systems computation conference*, 2011.

[8] T.H. Demiray. *Simulation of Power System Dynamics using Dynamic Phasor Models*. PhD thesis, ETH Zurich, 2008.

[9] T. M. Haileselassie and K. Uhlen. Power system security in a meshed north sea HVDC grid. *Proceedings of the IEEE*, 101(4):978–990, 2013.

[10] H. K. Khalil. *Nonlinear Systems*. Prentice Hall, 2002.

[11] P. Kundur. *Power System Stability and Control*. The Epri Power System Engineering. McGraw-Hill Companies,Incorporated, 1994.

[12] R. Li, S. Bozhko, and G. Asher. Frequency control design for offshore wind farm grid with LCC-HVDC link connection. *IEEE Transactions on Power Electronics*, 23(3):1085–1092, 2008.

[13] J. Machowski, J. W. Bialek, and J. R. Bumby. *Power System Dynamics: Stability and Control*. Wiley, 2008.

[14] Z. Melhem. *Electricity Transmission, Distribution and Storage Systems*. Woodhead Publishing Series in Energy. Elsevier Science, 2013.

[15] F. Milano. *Power System Modelling and Scripting*. Springer, 2010.

[16] K. R. Padiyar. *HVDC power transmission systems: technology and system interactions*. New Age International, 1990.

[17] B. Silva, C. L. Moreira, L. Seca, Y. Phulpin, and J. A. Peas Lopes. Provision of inertial and primary frequency control services using offshore multiterminal HVDC networks. *IEEE Transactions on Sustainable Energy*, 3(4):800–808, 2012.

[18] J. A. Taylor and L. Scardovi. Decentralized control of DC-segmented power systems.

[19] D. Van Hertem, M. Ghandhari, and M. Delimar. Technical limitations towards a SuperGrid - A European prospective. In *IEEE International Energy Conference and Exhibition*, pages 302–309, 2010.

[20] J. C. Willems. Dissipative dynamical systems part i: General theory. *Archive for rational mechanics and analysis*, 45(5):321–351, 1972.